

PaleoView3D: FROM SPECIMEN TO ONLINE DIGITAL MODEL

Nicholas E. Smith and Suzanne G. Strait

ABSTRACT

Recent technological advancements in 3D data acquisition and the ability to digitize museum collections have revolutionized the way one can access and visualize paleontological specimens. Instruments like high-resolution CT scanners and 3D laser scanners have simplified the digitization process, paving the way for 3D online museums.

The goals of this study were two-fold. First, to automate, standardize, and document the laser scanning/modeling technique used to generate models for one such database, PaleoView3D. Second, using PaleoView3D as a test case, to illustrate the necessity for other websites to include detailed error studies, modeling protocols, and associated metadata to facilitate the comparative use of online morphological data.

Automation and standardization were achieved by coating specimens with ammonium chloride, constructing a nine-specimen multiscan platform, and implementing an autosurfacing macro which combined reduced modeling time by 60%. An extensive error study was performed to test the accuracy of this technique using controls of known dimensions. The process was highly accurate in all three dimensions with percent errors of: 1D = 0.4%; 2D = 0.05%; 3D = 1.74%. Because many of the specimens digitized were casts, a molding/casting error study was also performed. First and second generation casts (i.e., a "cast of a cast") deviated from the original specimen a maximum of ± 0.074 mm and, as expected, variation increased slightly with subsequent generations. By standardizing and documenting the methodology and accuracy of this technique, researchers can make an informed decision concerning how to utilize models from PaleoView3D.

Nicholas E. Smith. Department of Biological Sciences, Marshall University, Huntington, West Virginia 25755, USA

* Present Address: Jackson School of Geosciences, The University of Texas at Austin, 1 University Station, C1140, Austin, Texas 78712-0254, USA. nick.smith@mail.utexas.edu

Suzanne G. Strait. Department of Biological Sciences, Marshall University, Huntington, West Virginia 25755, USA. straittho@marshall.edu

KEY WORDS: laser scanning; 3D models; PaleoView3D.org; fossil mammals; Paleocene; Eocene

INTRODUCTION

Technological advances have given paleonto-

logical researchers a variety of new methods for collecting 3D data, drastically changing how data

PE Article Number: 11.2.11A

Copyright: Society of Vertebrate Paleontology July 2008

Submission: 16 March 2008. Acceptance: 24 June 2008

Smith, Nicholas E. and Strait, Suzanne G. 2008. PaleoView3D: from Specimen to Online Digital Model. *Palaeontologia Electronica* Vol. 11, Issue 2; 11A:17p;

http://palaeo-electronica.org/2008_2/1134/index.html

are acquired and permitting novel, sophisticated 3D morphological analyses. High-resolution digitizers and scanners are unique in that the data they produce can be used to collect 3D data points from complex morphology, such as mammalian molars or tarsals. The Reflex Microscope was the first commonly available instrument for collecting 3D data on small- to medium-sized specimens (e.g., Strait 1993a, 1993b, 2001; Reed 1997; Yamashita 1998). However, this method cannot be broadly applied, as the researcher has to individually select each point to be recorded. This method is useful for comparisons of discrete landmarks and features, but it is too cumbersome and time consuming to collect the thousands of points necessary for accurate 3D characterization of even a single mammalian tooth. Furthermore, the low accuracy and resolution of electromagnetic (i.e., Polhemus 3Draw Pro) or contact digitizers (Immersion Microscribe 3D) (Zucotti 1998; Ungar and Williamson 2000; Wilhite 2003) make them impractical for working on all but the largest mammals. Confocal microscopy has also been used for 3D model generation of mammalian dental specimens (Jernvall and Selanne 1999; Evans et al. 2001) and is an excellent choice for very small specimens. However, since this technology was designed for biomedical imaging of tissues, cells, and organelles, it has specimen size limitations. Although specimens as large as 6 mm have been reported, those above 1-2 mm need to be scanned in pieces and merged, considerably increasing the processing time (Jernvall and Selanne 1999) and potential error.

Two methods have proven most beneficial for 3D data collection of complex morphology, Computed Tomography (CT) and 3D laser scanning. High-resolution x-ray CT scanners have proven to be a valuable technology for producing morphological models of vertebrates from a broad range of specimen sizes (e.g., DigiMorph; Kobayashi et al. 2002; Silcox 2003; Clifford and Witmer 2004; Kay et al. 2004; Colbert 2005; Dumont et al. 2005, 2006; Claeson et al. 2006; Holliday et al. 2006; Rayfield and Milner, 2006; Ridgely and Witmer 2006; Macrini et al. 2006). CT data can be very accurate (the degree of accuracy depends inherently on the CT scanning system) and is the only technology for obtaining internal data since it actually acquires sectional data through specimens. For collection of surface feature data laser scanners can also be used (3Dmuseum; Lyons et al. 2000; Motani 2005; Boyd and Motani 2006; Delson et al. 2006; Evans et al. 2006, 2007; Motani et al. 2006; Penkrot 2006; Rybczynski et al. 2006; Smith

and Strait 2006; Strait and Smith 2006; Wilson et al. 2006). Just like CT scanners, the precision of the models is scanner dependent but can produce surface models as equally detailed and accurate and are comparably time efficient when both scanning and processing are considered. The primary advantage of high-resolution laser scanners over CT scanners is that they are less expensive and require less technical expertise to operate and maintain.

Growing alongside the technology to produce 3D models is the computing power necessary to manipulate 3D data and the potential to make these models readily accessible via the Internet. The development of more online databases has also been driven by funding agencies, with increasing emphasis on the ability of researchers to disseminate data to peers, educators, and the general public. As a result, online databases have become increasingly important tools in biological and paleontological research, teaching, and outreach. Existing sites include compilations of vast amounts of data, in unique formats that are almost instantaneously accessible on the web (e.g., Carrasco et al. 2005; O'Leary and Kaufman 2007; North American Fossil Mammal Systematics Database 2002; The Paleobiology Database 1998; Maddison and Schulz 2007). Additionally, with the introduction of CT and laser scanners to paleontological studies, websites are also now available that feature 3D models of fossils. Sites such as 3D Museum (<http://www.3dmuseum.org>) provide visualization of a host of fossil taxa, and the Digital Morphology library (<http://www.digimorph.org>) houses many CT based models of extant and fossil vertebrates. The MorphoBrowser database (<http://morphobrowser.biocenter.helsinki.fi/>) specializes in vertebrate dental remains and includes a shape search function, to locate taxa of similar morphology (Evans et al. 2005). PaleoView3D (<http://paleoview3d.org>) is devoted to publishing 3D models and associated metadata of late Paleocene and early Eocene mammals (Strait and Smith 2006).

PaleoView3D is the first online site whose primary goal is not just to display 3D models of fossil organisms, but to allow users to download 3D data for their own research. During the development of PaleoView3D, several major issues had to be addressed: 1) how to standardize model production for consistency from model to model, 2) how to expedite the production of a large number of models, and 3) how to evaluate model accuracy. Standardization of methodology included consistent coating of specimens prior to scanning and during

the scanning process and the use of a consistent step-size (distance the laser travels between scan-lines) and sensor exposure settings. New methods were explored for expediting scanning and modeling included the development of a multiscan platform permitting multiple specimens to be scanned and registered in unison and designing an autosurfacing macro to facilitate image processing uniformity. Error studies were performed on objects of known dimension to assess model accuracy. Finally, since by necessity many of the PaleoView3D models were based on casts as opposed to original specimens, an error study was designed to compare models based on casts versus the originals.

While online 3D databases provide tremendous opportunity for paleontological analyses, certain precautions must be taken before incorporating 3D data from multiple sources. Unfortunately, not all 3D models are created equal due to the variety of aforementioned acquisition and modeling techniques. In order to comparatively analyze 3D models from PaleoView3D and other databases, users must have confidence in the accuracy of those models, and should be informed of the process used to generate those data. Therefore, rigorous testing and documentation of the modeling process is necessary prior to dissemination of these data, so that the user can make an informed decision on how best to utilize the models. The goal of this study was to standardize and document the novel modeling process used to generate models for PaleoView3D, in particular, with a broader implication of showing the necessity for the explication of model production and accuracy for all online databases.

MATERIALS AND METHODS

Laser Scanning and Data Acquisition

The laser scanner used in this study was a Surveyor RPS-120 probe (Laser Design Inc., Minneapolis, MN) mounted on a tri-axial automated stage (ISEL Automation, Eichenzell, Germany) (Figure 1). With this system, a red laser beam (620 nm wavelength) is emitted from the diode and spread passively into a laser plane (Figure 2.1). This laser



Figure 1. Laser scanning system consisting of a Laser Design Inc. RPS 120 probe mounted on an ISEL Automation computer numerical control (CNC) gantry unit.

plane appears as a line on the specimen and serves as the non-contact probe for the instrument (Figure 2.2). The laser line is reflected off the surface of the object and collected by dual optical sensors, charge coupled device (CCD) arrays similar to those found in digital cameras (Figure 2.1). As

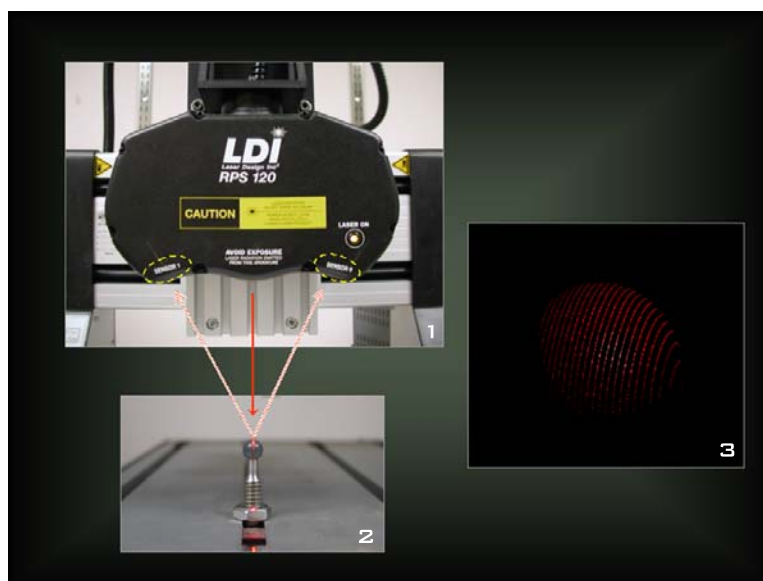


Figure 2. Schematic diagram of the laser scanning process. A laser beam is emitted from the diode in the unit and spread into a laser plane (1). The laser plane, appearing as a line on the sphere (2), is reflected and collected by dual CCD arrays (1). The resulting 2D profile is digitized and as the unit travels along the x-axis of the object, multiple profiles are collected yielding a 3D coordinate point cloud of the surface (3).

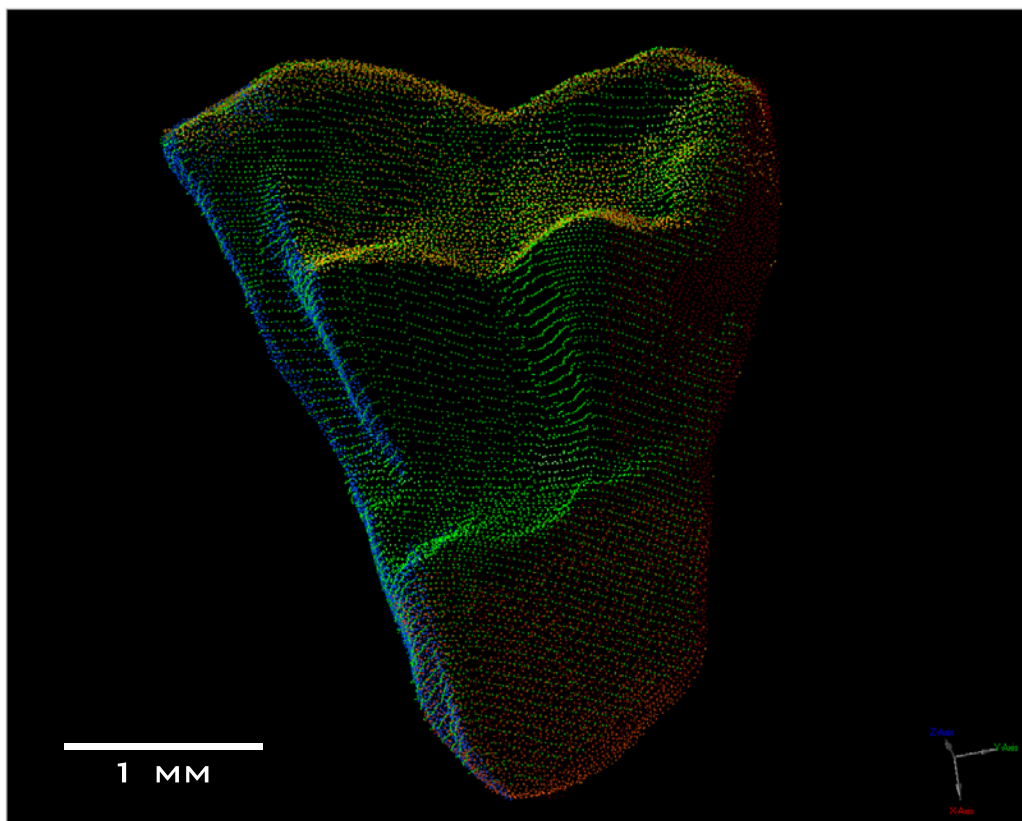


Figure 3. Point cloud of left M³ of *Mimoperadectes labrus* (UCMP 212703). Registered scan views representing the 3D surface are: occlusal (green); mesial (blue); distal (red); buccal (orange); and lingual (purple).

the stage moves the RPS (rapid profile scanning) unit over the specimen, the sensors collect a series of 2D profiles (scan-lines) of the object which collectively form a 3D coordinate point cloud of the surface (Figure 2.3).

Determining instrument resolution is not straightforward, because of its unique ability to incorporate multiple views of the same specimen. Therefore, maximum resolution can only be given per scan view. A single scan has a theoretical maximum resolution of 23.0 microns along the y-axis and 27.6 microns along the z-axis, each of which are determined by the dimensions of the CCD arrays. The resolution along the x-axis is dependent on the minimum interval (step-size) of the stage stepper motor which is 10 microns. To give an idea of surface point density, the probe has the ability to collect 480 points per scan-line with point spacing of 25 microns. As an example, the minimum number of points necessary to adequately cover the occlusal surface of a marsupial molar 1.5 mm in length is around 2,500 points (Figure 3). The software used to acquire the 3D data was Surveyor Scan Control v. 4.1.009 (Laser

Design Inc., Minneapolis, MN), which is an updated version of their proprietary Datasculpt software.

Specimen Coating

Unlike scanning electron microscopy in which high reflectivity is advantageous, the sensors in laser scanners require diffuse light. This proved especially problematic for dental specimens (or casts) because the high reflectivity of the enamel (or casting compound) caused the laser line to “shimmer” along the surface of the tooth. This created hotspots along the profile and yielded noisy point cloud data. To reduce the effects of this phenomenon, specimens were lightly dusted with an ammonium chloride (NH₄Cl) coating. Other compounds were tested (i.e., Spotcheck SKD-S2 Developer, Magnaflux, Glenview, IL; magnesium chloride) but ammonium chloride proved the lightest, most efficient, and easiest to remove. To coat a specimen, the ammonium chloride was heated and vaporized in a custom built glass instrument and then mouth-blown onto the surface of the specimen (Figure 4). All specimens were dusted



Figure 4. Coating a specimen with ammonium chloride (NH_4Cl). The compound is heated and vaporized in a glass instrument and then mouth-blown onto the surface of the specimen.

with the lightest possible coating, and visually examined for consistency prior to scanning. Although there is an element skill required for this method, a cautious technician can quickly learn the indications of undercoating (sparse, still semi-reflective areas; variations in color) and overcoating (thickened appearance; loss of morphological resolution). In most cases the compound can easily be dusted off with compressed air or a light brushing, and can be reapplied as necessary to achieve an even coating. As illustrated on a stainless steel scale bar, this coating was very effective in diffusing the laser light, and provided crisp reflections of the laser line (Figure 5). Beyond its diffusive effect, the specimen coating also enhanced the accuracy of the scans by yielding a consistent surface from one specimen to the next. Because variations in specimen color and texture have a profound effect on the laser's probe, the coating standardized the scan parameters and served to automate the process as well, by permitting the use of the same exposure settings for all specimens.

Specimen Scanning and Scan Parameters

Once coated, specimens were mounted to the stage for the first of five scans. By default, occlusal view was

chosen as the primary orientation of dental remains. Path plans (essentially the start and stop positions for data acquisition) were defined based on the dimensions of the specimen, and scan parameters (linear spacing and exposure) were configured. To determine the appropriate linear spacing (step-size for the stage stepper motor), multiple spacing trials (10, 20, 30, 50 μm) were conducted on isolated dental specimens of various size classes (< 4 mm in length; 4-8 mm; 8-12 mm; > 12 mm). Each resulting point cloud was examined for adequate surface coverage (point density) for the desired level of morphological resolution.



Figure 5. Reflection of the laser line along a stainless steel scale bar illustrating the necessity to coat reflective objects. The left half of the bar was left uncoated while the right side was lightly dusted with ammonium chloride.

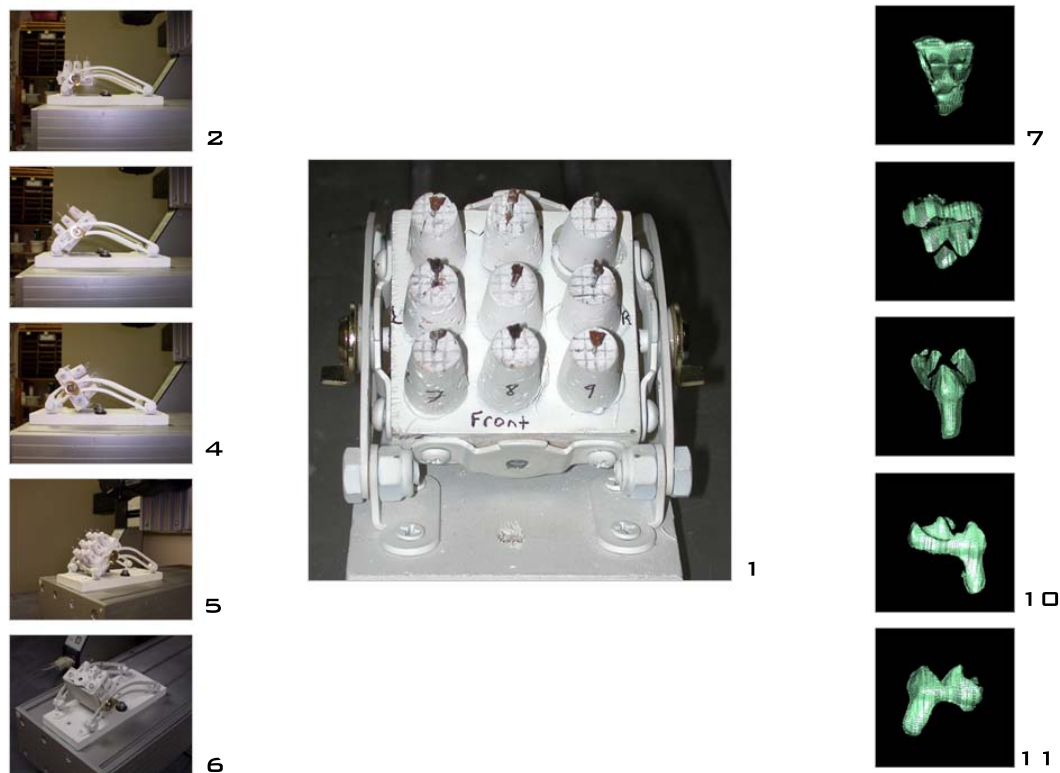


Figure 6. The multiscan platform with nine early Eocene marsupial molars (1). Figures 2-6 show the fixed stage positions for the five standard scan views. Figures 7-11 show representative point cloud data for each corresponding position: occlusal (7), buccal (8), lingual (9), mesial (10), and distal (11).

The general rule developed for determining appropriate linear spacing was:

- specimens < 4 mm in length: 10 μ m spacing
- specimens 4-8 mm in length: 20 μ m spacing
- specimens 8-12 mm in length: 30 μ m spacing
- specimens > 12 mm in length: 50 μ m spacing

Because all specimens were coated with ammonium chloride, the same exposure settings could be maintained. Based on the same principal as shutter speed in photography, exposure time in laser scanning is the duration (msec) that the CCD arrays are exposed to incoming photons. Underexposure yields little or no scan data, while overexposure leads to over-saturation and thus noisy scan data. Due to variation between the two sensor arrays, it was discovered that Sensor 0 must be set to a slightly longer exposure time to acquire comparable amounts of data. With the ammonium chloride coating, the exposure for Sensor 0 was set to 0.35 msec and Sensor 1 was set to 0.25 msec.

After all settings were configured, the surface point cloud data were collected and saved for a single scan orientation (view). To adequately cover the surface of a dental specimen, five views (occlusal, buccal, lingual, mesial, and distal) were typically required. The five resulting point clouds were saved as individual files, to later be registered into a cohesive model (Figure 3) during the registration process (described below).

Automation and Standardization of the Scanning and Modeling Process

Development of the Multiscan Platform. While the aforementioned scanning procedure was effective for scanning individual specimens, in order to expedite the modeling process, it was necessary to scan and render multiple specimens simultaneously. This was accomplished by the development of a nine-specimen multi-scan platform (Figure 6.1). Because all models for PaleoView3D are complete 3D surfaces, it was necessary to adopt a rotational scanning approach to ade-

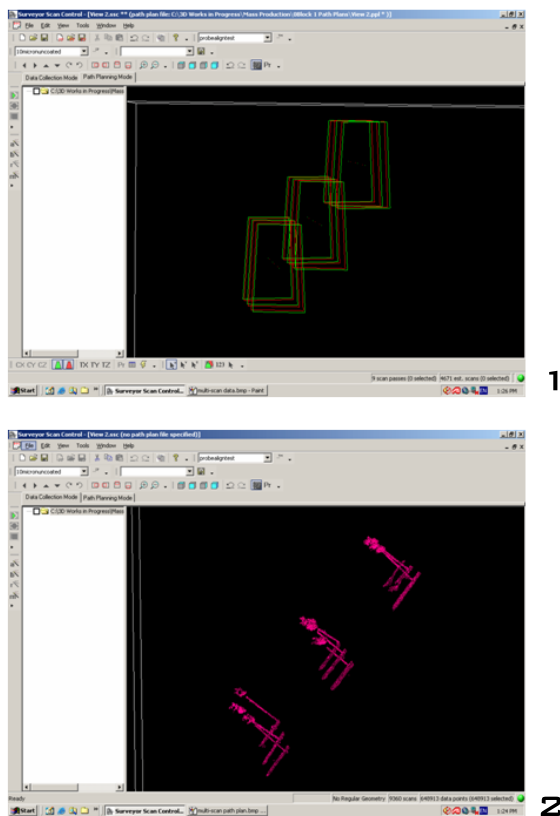


Figure 7. Lateral view of predefined path plans in Surveor Scan Control (1). Each green trapezoid represents a start position and each red trapezoid represents a stop position for the nine specimens of the multiscan platform (1). The corresponding specimen point clouds acquired via those path plans are highlighted in pink (2).

quately cover the entire surface of the specimens. Although complete automation of the scanning process would have been possible with a manufactured motorized rotary stage, integrating it into the existing system would have been expensive (~10,000 USD). Additionally, with the extra stage mount, the work envelope would also have been greatly reduced. Borrowing from rotary designs of existing stages, a low-cost (< 20 USD) multiscan platform was constructed and functions as a manual version of a rotary stage.

Because five views were required to adequately cover the surface of most specimens, five fixed stage positions were established (Figures 6.2-6.6). Representative scans for each corresponding position can be seen in Figure 6.7-6.11. Default path plans were defined for each stage position (Figure 7.1), automating a tedious process that can now be opened and run with a single command. Not only were the multiple specimens

scanned simultaneously, the resulting nine-specimen point cloud (Figure 7.2) was imported into Geomagic Studio 6.0 and processed in unison. This bolt-on specimen holder permitted simultaneous scanning of up to nine small (< 5 mm) specimens. The nine specimen platform was chosen because the 3 x 3 design was the maximum size square that would fit within the work envelope without shading lower specimens when the stage was tilted. The stage mount and the platform (to which the specimens were affixed) were constructed of wood, and the mounting brackets were modified lid support hinge rails. Four brackets were mounted to the platform, one on each side so that it could be bolted down to the support rails at the desired angle of inclination. Standard specimen mounting corks were glued to the platform, and the mounting pins were inserted into the corks, permitting easy transfer of specimens.

Manual Registration. Scans of all five orientations and the resulting point clouds were then imported into Geomagic Studio 6.0 (Raindrop Inc., Durham, NC) for registration (the alignment of multiple views) (Figure 8). All registrations were performed in Studio 6.0 because of a software glitch that was discovered in later versions of the program (Studio 7.0-10.0) that impaired the registration process for small (< 10 mm) specimens. This step was probably the most important of the modeling process, as it united the five scans into a single 3D point cloud. To perform the operation a minimum of three (x, y, z) points were selected on one model, and three corresponding points were selected on the second model. Points chosen were well-defined morphological structures (such as a cusp tip) that were widely dispersed on the specimen. The “Register” algorithm was applied, and the two surfaces were aligned (Figure 8). The same process was applied with this new merged object and each remaining view. Once registered, each specimen was saved individually, and subsequent operations were performed on isolated models.

Autosurfacing Macro. Several post-registration smoothing functions (e.g., removal of outliers, uniform sampling, etc...) were performed in Studio, and the point cloud was wrapped with a polygonal surface. The processing phase of the technique was the most demanding, required the most amount of training, and was thus the largest source of human error. Any number of processing functions (e.g., Noise Reduction, Smooth, Select Outliers, etc...) can over-smooth the model and greatly alter the morphology of the specimen. To minimize error and standardize the modeling process, an

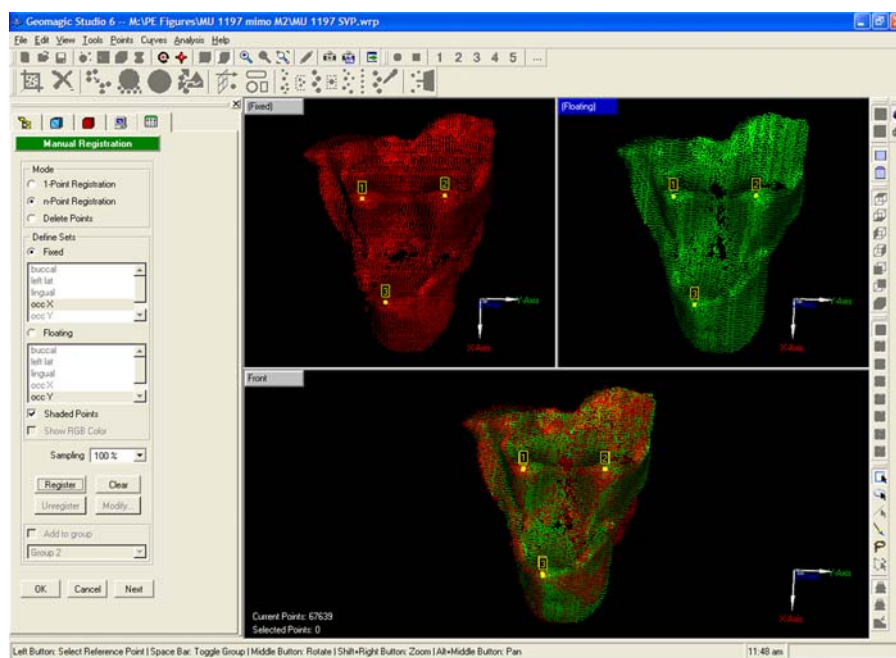


Figure 8. Video capture of the manual registration process in Geomagic Studio. Three corresponding points are selected on each model, roughly aligning the two scans. The registration algorithm is then applied to find the best fit of the two models.

autosurfacing macro was developed in Geomagic Studio and is available for download at <http://www.paleoview3d.org>. Creating the macro was straightforward, all desired operations and corresponding parameters were performed on an initial model and recorded in the macro as an automated file. To use the autosurfacing macro, the file is simply loaded and run with a single command, and all pre-programmed operations are applied to the current point cloud (Figure 9).

Morphometric Error Study

Because PaleoView3D models are available for public access and may be downloaded for use in morphometric applications, it was imperative that each accurately represented the original specimen. To illustrate the accuracy and precision of this new laser scanning technique, an extensive error study was performed in all three Cartesian axes. It should be noted that in each of the studies, the modeling process was repeated with consistent parameters in its entirety: coating, scanning, registration, and surface rendering (via the newly developed autosurfacing macro when applicable).

Linear (1D) Error Study. Linear measurements are undoubtedly the easiest to acquire, and 1D data are still widely used in paleontological applications. Because this technique was designed for small organic specimens of various morphologies,

selection of an appropriate control object was key in assessing the linear accuracy of the modeling process. A small (5.5 mm) machine tooled screw with a known thread-pitch (essentially the wavelength of the threads) of 0.250 mm was chosen as the control (Figure 10). The screw was scanned (0.01 mm linear spacing) and modeled from start to finish three separate times on independent days. Each model was composed of five scan views and rendered using the autosurfacing macro. Ten crest to crest linear measurements were taken per model using the “DimLinear” tool in AutoCAD 2005 (Figure 10).

Surface Area (2D) Error Study. To incorporate the second dimension into the study, the control object chosen was a one decimeter scale bar with known dimensions of 100 x 10 x 1 mm (Figure 11). The surfaces of this scale bar were ideal for calculating the 2D area, and one long side (100 x 10 mm) was scanned and modeled three separate times. Because only a single scan view was used in model creation, the autosurfacing macro could not be utilized in this assessment. The surface area of the models was measured using the “Calculate Volumes” command in 3D-Doctor, which also yields surface area data. Since this measurement is a single command, the only source of human error is in the modeling process. Scans were main-

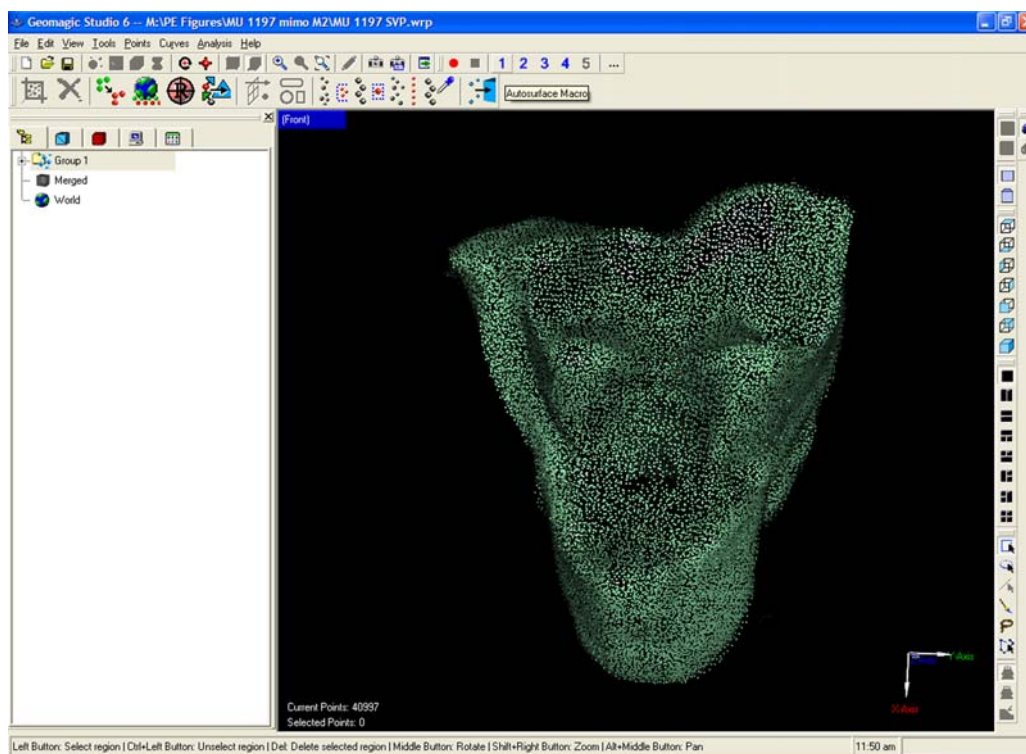


Figure 9. Video capture of the autosurfacing macro applied to an upper molar of *Mimoperadectes labrus*. Once the five views have been registered manually, this automated surfacing is performed with a single command. In this example, the macro is followed by an additional smoothing function.

tained at the highest resolution (0.01 mm) to remain consistent with the linear error study.

Volumetric (3D) Error Study. The same scale bar used in the surface area study was modeled for the volumetric analysis (Figure 11). This scale bar has a known volume of 1000 cubic millimeters (100 mm x 10 mm x 1 mm). Modeling this object proved difficult due to the 1 mm thickness in the z-axis. When attempting to employ the global registration, the software would consistently attempt to register the opposing broad surfaces as a single surface. For this reason the autosurfacing macro was not used, but all steps and parameters were maintained minus the global registration. Three separate models were generated duplicating the entire process, registering six different scan views per model. The volumes were calculated in Geomagic Studio 6.0 using the “Compute Volume” analysis and cross checked in 3D-Doctor using the “Calculate Volumes” command. As with the 2D study, there was no potential source of human error in the measurement.

Casting Error Study

Because the goal of PaleoView3D is to digitize the types of Paleocene-Eocene taxa, speci-

mens from many museums were involved in the process. Original specimens were scanned whenever possible; however, casts were also used since many museums are hesitant to loan original type material. Additionally, the type specimens of some species have been lost or damaged, so that casts are the only option. In some cases where types are lost or fragile, some museums are molding casts of earlier casts for loans. Given the use of casts for PaleoView3D scans, it was necessary to assess the accuracy of the molding/casting process. Although manufacturers publish shrinkage rates, few studies (Evans et al. 2001) have documented shrinkage rates for a single molding and casting procedure. Furthermore, there has been no assessment of the error of cumulative casting procedures. Therefore, it was necessary to examine the variation between the cast and the original specimen, as well as any “casts of casts.”

To address this issue, an isolated upper molar of an early Eocene creodont, *Arfia junnei* (UCMP 216155), was modeled using the laser scanning process. This specimen was then molded using Dow Corning HS III RTV Silicone and cast with TAP Plastics Four to One epoxy resin. The published shrinkage rates at 24 hours for these

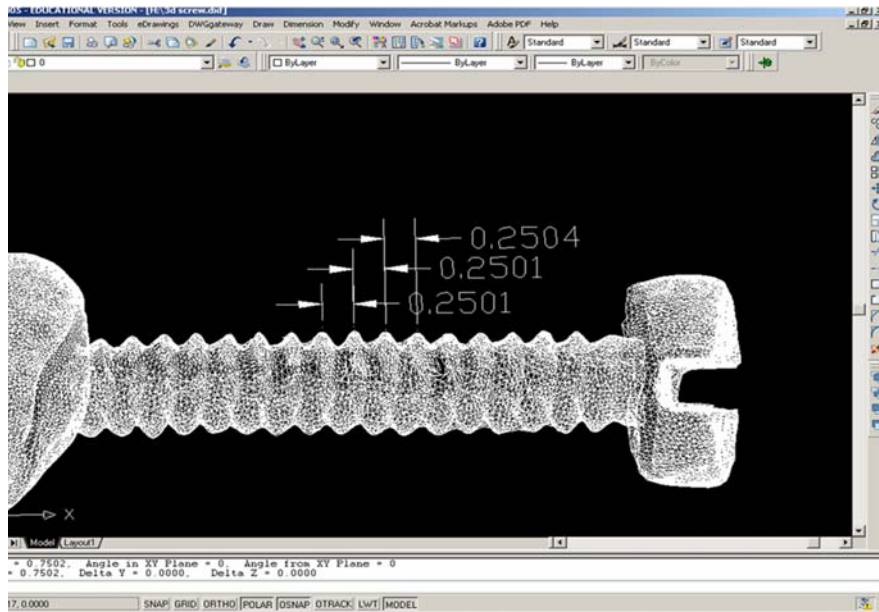


Figure 10. Three-dimensional model of the machined screw used as the control object for the linear study. Taken in AutoCAD 2005, three crest-to-crest linear measurements (mm) are shown. The known thread pitch for this screw was 0.250 mm.

compounds are 0.2% and < 1.0%, respectively. This first generation cast was then scanned and rendered using the same technique. Once scanned, the molding and casting process was repeated using the first generation cast, essentially making a “cast of a cast.” This process was performed twice more concluding with a fourth generation cast. Variation between the resulting models was assessed using the 3D Compare operation in

Geomagic Studio 6.0. This operation generates a color-coded spectrum model illustrating areas of correspondence and deviation between the two surfaces (Figure 12). Areas of the resulting spectrum model that appear green illustrate regions of highest correspondence and in this study, deviate less than ± 0.018 mm from one another. By default, surfaces at the higher end of the spectrum (yellows and reds) highlight areas in which the second

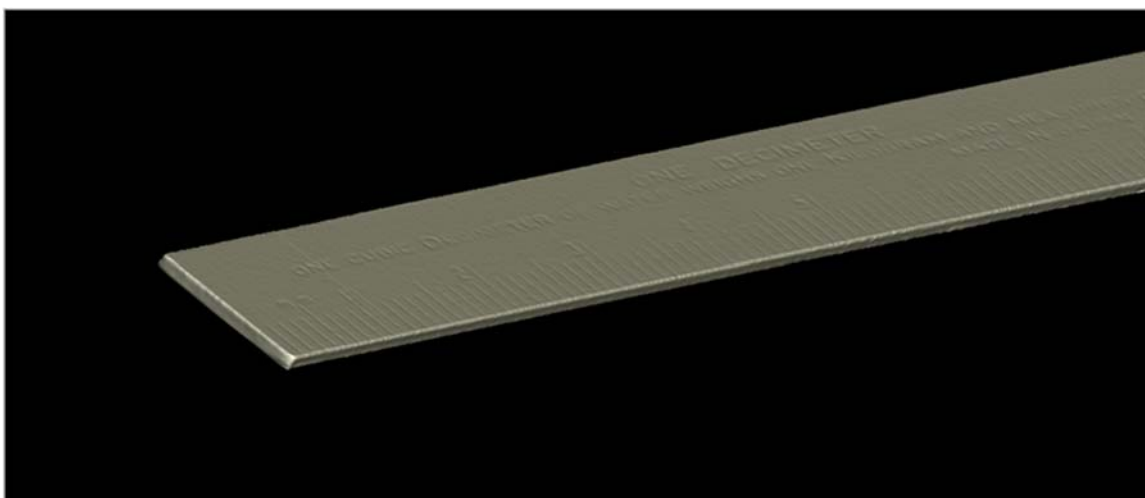


Figure 11. Screen capture of the resulting scale bar model used in the 2D and 3D error study. The dimensions of the scale bar were 100 x 10 x 1 mm.

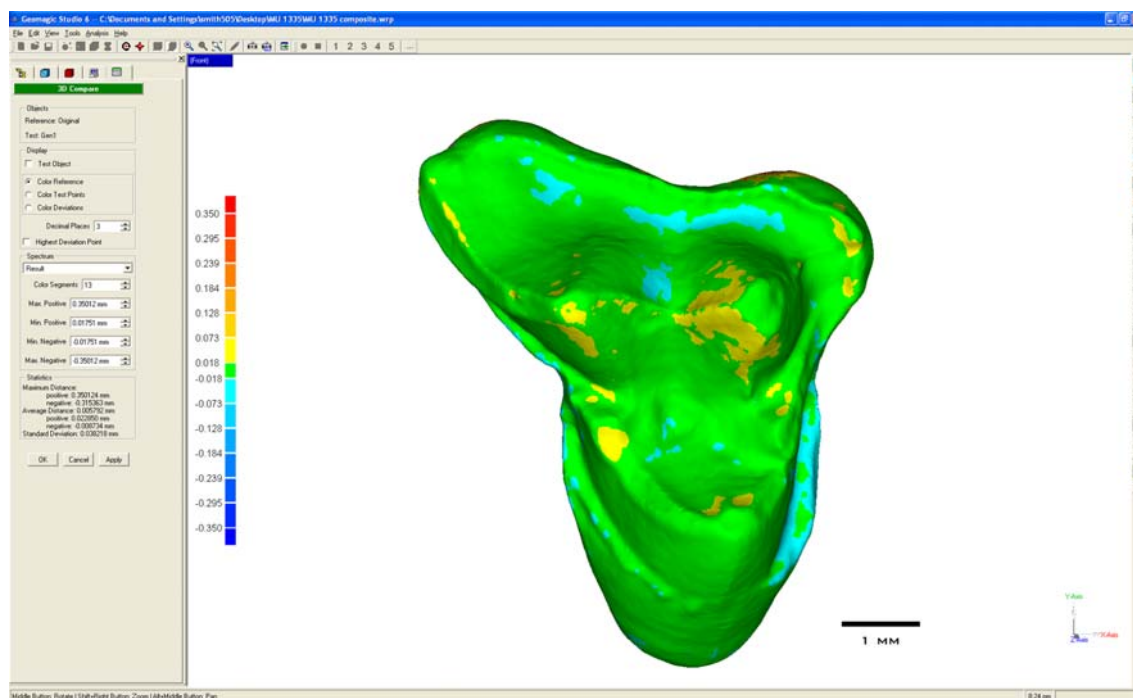


Figure 12. Screen capture of the 3D compare function in Geomagic Studio that highlights regions of correspondence and deviation between the two models of an *Arfia junnei* upper molar (UCMP 216155). Surfaces shown in green deviate less than ± 0.018 mm from one another while blues and reds represent regions of positive and negative relief, respectively.

model has positive relief, i.e., is larger than the original. Those surfaces colored at the lower end of the spectrum (blues and violets) highlight areas of negative relief, or places where the second model is smaller than the original. Because the epoxy is known to shrink, some variation will be introduced simply in the alignment of the models compared. Since we were examining the effects of casting on overall morphology, we chose not to scale the models, but to compare them as produced.

RESULTS

Development of the Multiscan Platform

The first result of this study was the design and implementation of the low-cost multiscan platform (Figure 6.1). Implementation of this device permitted simultaneous scanning of up to nine specimens and because each of the five stage positions were fixed (Figures 6.2-6.6), generic path plans were defined for each of the five scan views (Figures 6.7-6.11). With this device, once the specimens were mounted to the platform, the pre-defined path plans were loaded and run with a single-click for each respective stage position (Figure 7). By reusing the pre-defined path plans, modeling

time was reduced by around 20%. Another advantage of using this in-house device was the level of accuracy maintained. Because the stage positions were fixed, there was no opportunity for added error (~ 0.02 mm) from the stage positioning system as would be seen with a motorized rotary unit.

Development of the Autosurfacing Macro

Another result of this study was the development of an autosurfacing macro. By using the autosurfacing macro, once all five views are registered manually, the rest of the process can be performed with a single command (Figure 9). This is especially advantageous, as it permits for uniformity of image processing and reduces human error.

Six commands were incorporated into the autosurfacing macro: Global Registration, Select Disconnected Components, Select Outliers, Uniform Sample, Merge, and Clean.

1. **Global Registration.** The Global Registration command essentially recalculates the fit of the individual point/polygon models and repositions them to form a more cohesive surface. This function is similar to the Manual Registration operation except that the registration

algorithm is applied to all five views simultaneously.

2. **Select Disconnected Components.** Incorporated more for specimens with multiple elements, the Select Disconnected Components command automatically selects those points (or clusters of points) that are spatially separated from the majority of the other points (cumulative percentage). These clusters are essentially those points that lie outside the potential surface boundary. Each cluster is calculated as a percentage of the total object, and a conservative sensitivity is programmed into the macro which selects those points that make up less than 5% of the total number of points.
3. **3) Select Outliers.** Similar to the Select Disconnected Components command, the Select Outliers function automatically detects and selects all points that lie outside the range of the majority of points. More sensitive than the former, this operation selects those points that lie outside a given range. To maintain morphological accuracy, it was determined by trial and error that the sensitivity level needed to be set to 66.6/100 in the autosurfacing macro. Levels set above this default setting cause the function to be too aggressive in removing outliers, and levels set below fail to adequately remove noisy data.
4. **Uniform Sample.** The Uniform Sample operation is derived from the curvature based sampling which reduces the number of points along a planar surface uniformly, but reduces those along curved edges based upon a predetermined density. This helps to preserve the natural curvature of an object, while reducing redundant points along the flatter surfaces of the specimen. The Uniform Sample function within the macro is set to reduce the number of points so that the absolute spacing between each point is 0.039 mm. In addition to greatly reducing file size, this function also serves to reduce surface noise.
5. **Merge.** The Merge function is basically a macro in itself, combining: Merge Points, Reduce Noise, Uniform Sample, and Wrap functions. The Merge Points operation combines all point objects into a single object (e.g., the standard five views of a specimen will be merged into a single point cloud). The Reduce Noise operation is employed conservatively in the macro as it has a tendency to

over-smooth potentially diagnostic morphologies. The Uniform Sample command was previously described and is not repeated in the macro. The Wrap function is the primary operation responsible for the transformation of the coordinate point cloud into a polygonal mesh surface model.

Morphometric Error Study

Linear (1D) Error Study. The resulting mean thread-pitch (known = 0.25 mm) from 30 measurements of the screw was 0.251 mm with a percent error of 0.4%. This slight overestimation is most likely attributed to the layer of ammonium chloride used to coat the object. The linear accuracy was calculated as ± 0.001 mm, and the repeatability was ± 0.0005 mm. With single micron scale accuracy, these results far surpass the manufacturer's stated claim of ± 0.00635 mm.

Surface Area (2D) Error Study. The resulting three area measurements taken from the scale bar (known = 1000 mm²) were: 998.04, 997.71, and 1002.67 mm². The mean calculated surface area was 999.47 mm² a percent error of 0.05%. The slight underestimation could partially be explained by an optical phenomenon that occurs at the edge of an object, when the angle of incidence of the laser plane exceeds 70 degrees from normal. This alters the perceived thickness of the laser line that makes it difficult for the software to delineate the true edge of the object. Because a single surface scan was used, this edge was most likely removed as noise in post-processing.

Volumetric (3D) Error Study. Both programs (Geomagic Studio 6.0 and 3D-Doctor) used to calculate the volume (known = 1000 mm³) of the three models of the scale bar yielded identical values per model: 1007.54, 1019.89, and 1026.15 mm³. The mean calculated volume was 1017.86 mm³ a percent error of 1.79%. The consistent slight overestimation is again most likely attributable to the ammonium chloride coating.

Casting Error Study

Comparison of the original specimen to the first generation cast showed the majority of the surface on the two models to be in correspondence, as illustrated by the green areas in Figure 13.1. Areas of highest deviation were concentrated along the cusps and posterior margins of the tooth, and the maximum deviation was in the range of ± 0.018 mm to ± 0.073 mm. The second generation cast varied from the original specimen a maximum

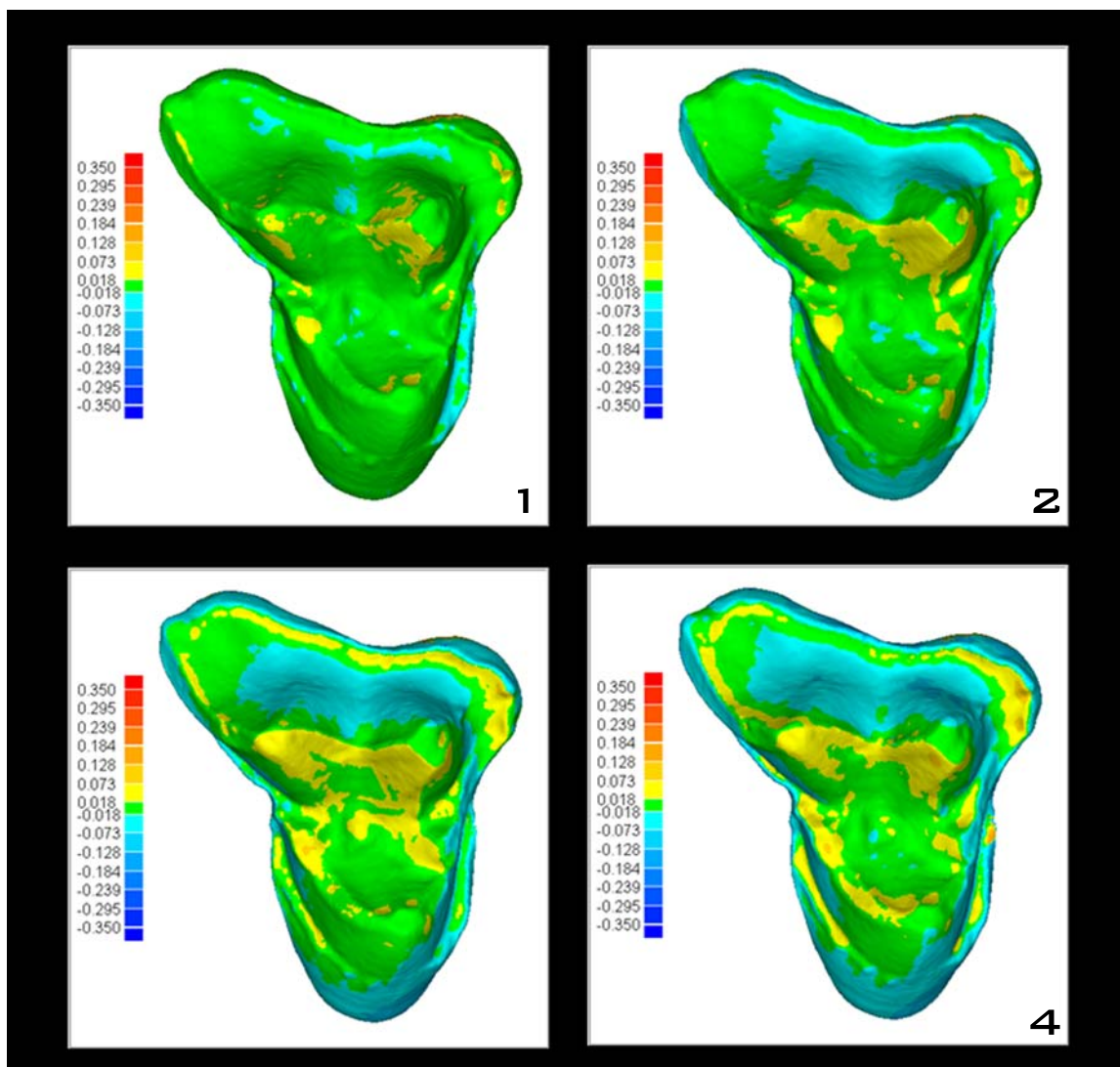


Figure 13. Results of the 3D comparison for the casting error study. The model of the original specimen was compared to the models of the first generation cast (1), second generation cast (2), third generation cast (3), and fourth generation cast (4).

of ± 0.018 mm to ± 0.073 mm, with most of the variation around the cusps and the styler shelf (Figure 13.2). With the third generation of molding/casting, increasing regions of negative relief (blue) appeared on the styler shelf and peripheral margins of the tooth (Figure 13.3). The maximum deviation between the original and the third generation cast ranged from ± 0.073 mm to ± 0.128 mm. The fourth and final molding/casting generation showed a greater increase in negative deviation along the outer margins of the tooth (Figure 13.4). Compared to the original specimen, this model yielded a maximum deviation of ± 0.073 mm to ± 0.128 mm.

CONCLUSION AND DISCUSSION

This paper focused on presenting methods that could further aid in the documentation and development of online 3D databases, using PaleoView3D as a case study. The majority of online sites that specialize in 3D morphological models are designed primarily as online museums, for housing and visual comparison of models (e.g., 3D Museum, DigiMorph, MorphoBrowser, and Naturalis). DigiMorph does offer downloadable 3D STL files for only 2% of its mammals, but this is obviously not the primary goal of this website. In order for the continued growth of websites that offer downloadable data, there needs to be confidence

within the user-base that these data conform to their research standards. Researchers need to know the accuracy and quality of the data represented on these sites; therefore, database developers must standardize how models are produced and publish data on how models were created so that the users know potential sources and degrees of error.

Standardization of models was achieved by consistently coating specimens with ammonium chloride. Aside from noise reduction caused by reflectivity, this permitted standardization of scan parameters and laser exposure settings. New methods were also developed to expedite and semi-automate data collection. Unlike with CT model production, scanning time can often be more time intensive than image processing. Therefore, with the number (~750) and variety of specimens (dental, cranial, and post-cranial) to be included in PaleoView3D it is imperative to develop a scanning technique that could more efficiently and accurately generate 3D models of the specimens. Implementation of the multiscan platform and macro reduced total modeling time (coating, scanning, registration, surfacing) by approximately 60% over traditional single scans. Model generation for nine isolated specimens (maximum held by platform) now takes an average of 5.5 hours (approximately 35 min per specimen) from start to finish. Using the predefined path plans, however, once a scan has been initiated, the user is free to process previously scanned data, maximizing efficiency. Because the focus of this website was not just model viewing, but producing data to be employed in morphometric analyses, it was also a requirement that these models maintain the highest degree of morphological accuracy. A multiscan platform that permitted nine specimens to be scanned (and therefore registered) at once was designed and implemented. Although this in-house model did not have the motorized rotation offered on many manufactured stages, it greatly reduced scan and registration time, at a much lower cost (~20 as opposed to ~10,000 USD), allowed for a larger work area, and was more accurate.

The image processing phase of 3D model development has the highest potential for the introduction of human error that could affect the accuracy and precision of models. Additionally, PaleoView3D is being developed at Marshall University, a primarily undergraduate institution, and the many technicians employed for the project are undergraduates with limited experience and short tenures. Therefore, another task was to make the

image processing as user-friendly and automated as possible to reduce sources of error and to facilitate image processing uniformity. After specimens are registered, it is now possible to surface specimens with a single command. The autosurfacing macro that was developed includes steps that checks the manual registration process, removes noise and extreme outliers, reduces redundant points and thereby greatly reducing file size, merges the point clouds from the multiple scans, and finally “wraps” the merged point cloud into a polygonal mesh to achieve the final model. Undergraduates, in as early as their second or sophomore year, have been successfully trained to independently scan and process models.

Finally, since by necessity many of the PaleoView3D models were based on casts as opposed to original specimens, an error study was designed to compare models based on casts versus original specimens. The casting error study demonstrated, as expected, that subsequent casting generations exhibit amplified shrinkage and do vary slightly from the original specimen. In addition to the error incurred by multiple molding and casting generations, error from the scanning and modeling processes were also incorporated, making this a “worst case scenario” repeatability study. Examining the maximum range of deviation (± 0.073 mm), for the first and second generation casts, these results are considered acceptable for most morphometric analyses. The maximum variation for the third and fourth generation casts (± 0.128 mm) is certainly less desirable, but this an extreme example, and most researchers would avoid analyzing a fourth generation cast even using traditional methods. It should be noted that the goal of this study was not to show whether this modeling process was more or less accurate than any other technique, but to document the results so that the user can decide how to best utilize these data. The error studies performed on objects of known dimensions suggest that these digital models are highly accurate. The 1D study of linear accuracy resulted in a 0.4% error rate, the 2D surface area error rate was 0.05%, and the 3D or volumetric error rate was 1.79%. Manufacturers include theoretical numbers that represent the maximal possible accuracy of their instruments; however, these typically not do include a combination of potential error rate for both scanning and modeling. Analogous studies are not available to contrast how this scanner and scanning protocol compare to other systems. However, the importance is that, with this study, researchers wishing to include

PaleoView3D models into their research will be aware of the error inherent in the models so they can take this into consideration when designing measurement and statistical options.

In order to gain a successful user-base and promote the sharing of data online, websites also need to be explicated concerning the sources of the data they publish. For example, associated with each PaleoView3D model is a list of technical specifications under which that model was produced including: the number of scans used to produce the model, whether a fossil or cast was scanned, what type of coating was applied to the specimen prior to scanning, the step-size or linear spacing between scans, the laser exposure time, the number of polygons that are included in the model, and the number of points that were used to derive a model. Association of these metadata with the models helps one assess the compatibility of data from multiple databases.

Due to the potential for growth of online 3D databases, we advocate the standardization of methods within sites, reporting of methodological error rates, and also explicitly documenting 3D model production protocols. By thoroughly documenting this information for PaleoView3D, we have given the user the ability to decide whether or not these data are acceptable for a particular study. We encourage all online 3D databases (present and future) to follow this approach of standardization and detailed documentation of modeling procedures, to promote the dissemination of 3D data useful for comparative analyses of paleontological specimens.

ACKNOWLEDGMENTS

We would like to thank M.J. Adkins and T. Penkrot, for assistance in specimen scanning and modeling and C. Xue for database and website development. We also acknowledge D. Neff for his immense help in establishment and operational training of the laser scanner and accompanying software. We thank P. Holroyd (University of California Museum of Paleontology) for use of specimens in this project. We also thank two anonymous reviewers for insightful comments that improved this manuscript. This project was funded by the National Science Foundation (DEB - Biotic Surveys & Inventories 020828; DBI - Biological Databases and Informatics 0543414), Marshall University, and NASA.

REFERENCES

- Boyd, A., and Motani, R. 2006. 3D Re-evaluation of the deformation removal technique based on jigsaw puzzling. *Journal of Vertebrate Paleontology*, 26(3), Supplement, 44-45A.
- Carrasco, M.A., Kraatz, B.P., Davis, E.B., and Barnosky, A.D. 2005. Miocene Mammal Mapping Project (MIOMAP). University of California Museum of Paleontology <http://www.ucmp.berkeley.edu/miomap/>.
- Claeson, K., Lundberg, J., and Hagadorn, W. 2006. Anatomy of the very tiny: Tomographic insights into morphology of extinct and extant fishes. *Journal of Vertebrate Paleontology*, 26(3), Supplement, 50A.
- Clifford, A.B., and Witmer, L.M. 2004. Case studies in novel narial anatomy: 3. Structure and function of the nasal cavity of saiga (Artiodactyla: Bovidae: *Saiga tatarica*). *Journal of Zoology, London* 264:217-230.
- Colbert, M.W. 2005. The Facial Skeleton of the Early Oligocene Colodon (Perissodactyla, Tapiroidea), *Palaentologia Electronica*, Vol. 8, Issue 1; 12A:27p, 600KB; http://paleo-electronica.org/paleo/2005_1/colbert12/issue1_05.htm
- Delson, E., Wiley, D., Harcourt-Smith, W., Frost, S., and Robsenberger, A. 2006. 3D approaches in paleoanthropology using geometric morphometrics and laser scanning. *Journal of Vertebrate Paleontology*, 26(3), Supplement, 55-56A.
- DigiMorph (The Digital Morphology Library). (online) Rowe, T. (Dir.). 2002-2005. The University of Texas at Austin <<http://digimorph.org/>>.
- Dumont, E.R., Piccirillo, J., and Grosse, I.R. 2005. Finite-element analysis of biting behavior and bone stress in the facial skeleton of bats. *The Anatomical Record*, Part A 283A:319-330.
- Dumont, E., Werle, S., and Grosse, I. 2006. 3D imaging and biomechanics: Bringing 3D finite element modeling to comparative biology. *Journal of Vertebrate Paleontology*, 26(3), Supplement, 57A.
- Evans, A.R., Harper, I.S., and Sanson, G.D. 2001. Confocal imaging, visualization, and 3-D surface measurement of small mammalian teeth. *Journal of Microscopy*, 204(2):108-119.
- Evans, A., Martin, T., Fortelius, M., and Jervall, J. 2006. Reconstructing dental occlusion in 3D: from carnivorans to *Asfaltomylos*. *Journal of Vertebrate Paleontology*, 26(3), Supplement, 59A.
- Evans, A.R., Wilson, G.P., Fortelius, M., and Jernvall, J. 2007. High-level similarity of dentitions in carnivorans and rodents. *Nature*, 445:78-81.
- Evans, G., Evans, A., Pljusnin, I., Fortelius, M., and Jernvall, J. 2005. MorphoBrowser—a new database for surfing the dental morphospace. *Journal of Vertebrate Paleontology*, 25(3), Supplement, 54A.
- Holliday, C.M., Ridgely, R.C., Balanoff, A.M., and Witmer, L.M. 2006. Cephalic vascular anatomy in flamingos (*Phoenicopterus ruber*) based on novel vascular injection and computed tomographic imaging analyses. *Anatomical Record*, Part A, 288A:1031-1041.

- Jernvall, J., and Selanne, L. 1999. Laser confocal microscopy and geographic information systems in the study of dental morphology. *Palaeontologia Electronica* Vol. 2, Issue 1:18, 905KB; http://palaeo-electronica.org/1999_1/confocal/issue1_99.htm
- Kay, R.F., Campbell, V.M., Rossie, J.V., Colbert, M.W., and Rowe, T.B. 2004. Olfactory fossa of *Tremacebus harringtoni* (Platyrrhini, Early Miocene, Sacanana, Argentina): Implications for activity pattern. *The Anatomical Record*, Part A, 281A:1157-1172.
- Kobayashi, Y., Winkler, D.A., and Jacobs, L.L. 2002. Origin of the tooth-replacement pattern in therian mammals: Evidence from a 110 myr old fossil. *Proceedings of the Royal Society of London*, B, 269:369-373.
- Lyons, P.D., Rioux, M., and Patterson, R.T. 2000. Application of a Three-Dimensional Color Laser Scanner to Paleontology: an Interactive Model of a Juvenile *Tylosaurus* sp. Basisphenoid-Basioccipital. *Palaeontologia Electronica*, Vol. 3, Issue 2, 4:16p., 2.04MB; http://palaeo-electronica.org/2000_2/neural/issue2_00.htm
- Macrini, T., Rowe, T., and Archer, M. 2006. Description of a cranial endocast from a fossil platypus, *Obdurodon dicksoni* (Monotremata, Ornithorhynchidae), and the relevance of endocranial characters to monotreme monophyly. *Journal of Morphology*, 267(8):1000-1015.
- Maddison, D.R., and Schulz, K.S. (eds.) 2007. *The Tree of Life Web Project*. <http://tolweb.org>.
- MorphoBrowser*. (online) Jernvall, J. (Dir.) 2003-2005. University of Helsinki. <http://morphobrowser.biocenter.helsinki.fi/>
- Motani, R. 2005. Detailed tooth morphology in a durophagous ichthyosaur captured by 3D laser scanner. *Journal of Vertebrate Paleontology*, 25(2):462-465.
- Motani, R., Milner, A., and Schmitz, L. 2006. The first truly objective method for 3D removal of geological deformation with an application to the braincase of *Archaeopteryx*. *Journal of Vertebrate Paleontology*, 26(3), Supplement, 103A.
- Naturalis*. (online) van Hengstum, R.J.M. (Dir.) 2005. Dutch National Museum of Natural History <<http://nlbif.eti.uva.nl/naturalis/>>.
- North American Fossil Mammal Systematics Database*. (online) Alroy J. (Dir.). 2002. UC Santa Barbara <<http://www.nceas.ucsb.edu/~alroy/nafmsd.html>>.
- O'Leary, M.A., and Kaufman, S.G. 2007. MorphoBank 2.5: Web application for morphological phylogenetics and taxonomy. <http://www.morphobank.org>
- PaleoView3D*. (online) Strait, S.G. (Dir.). 2005. Marshall University <<http://paleoview3d.marshall.edu/>>.
- The Paleobiology Database*. (online) Alroy, J. (Dir.) 1998. NCEAS UC Santa Barbara <<http://paleodb.org>>.
- Penkrot, T. 2006. Comparative paleoecologies of North American mioclaenids and "hyposodontids" (Mammalia: "Condylarthra") using combined dental morphometric techniques. *Journal of Vertebrate Paleontology*, 26(3), Supplement, 109A.
- Rayfield, E., and Milner, A. 2006. The evolution of piscivory in theropod dinosaurs. *Journal of Vertebrate Paleontology*, 26(3): Supplement, 114A.
- Reed, D.N.O. 1997. Contour mapping as a new method for interpreting diet from tooth morphology. *American Journal of Physical Anthropology*, Supplement 24:194.
- Ridgely, R., and Witmer, L. 2006. Dead on arrival: Optimizing CT data acquisition of fossils using modern hospital CT scanners. *Journal of Vertebrate Paleontology*, 26(3), Supplement, 115A.
- Rybczynski, N., Tirabasso, A., Cuthbertson, R., and Holliday, C. 2006. A 3D cranial animation of *Edmontosaurus* for testing feeding hypotheses. *Journal of Vertebrate Paleontology*, 26(3), Supplement, 177A.
- Silcox, M.T. 2003. New discoveries on the middle ear anatomy of *Ignacius graybullianus* (Paramomyidae, Primates) from ultra high resolution X-ray computed tomography. *Journal of Human Evolution*, 44(1):73-86.
- Smith, N.E., and Strait, S.G. 2006. Laser scanning automation and standardization. *Journal of Vertebrate Paleontology*, 26(3), Supplement, 127A.
- Strait, S.G. 1993a. Differences in occlusal morphology and molar size in frugivores and faunivores. *Journal of Human Evolution*, 25:471-484.
- Strait, S.G. 1993b. Molar morphology and food texture among small-bodied insectivorous mammals. *Journal of Mammalogy*, 74(2):391-402.
- Strait, S.G. 2001. Dietary reconstruction in small-bodied omomyoid primates. *Journal of Vertebrate Paleontology*, 21(2):322-334.
- Strait, S.G., and Smith, N.E. 2006. PaleoView3D: An interactive database of mammals from the Paleocene/Eocene boundary. *Journal of Vertebrate Paleontology*, 26(3), Supplement, 129A.
- 3D Museum*. (online) Motani, R. (Dir.). 2004. UC Davis <http://www.3dmuseum.org>
- Ungar, P., and Williamson, M. 2000. Exploring the effects of tooth wear on functional morphology: A preliminary study using dental topographic analysis. *Palaeontologia electronica*, Vol. 3, Issue 1; 1:18 pp., 752KB; http://palaeo-electronica.org/2000_1/gorilla/issue1_00.htm.
- Wilhite, R. 2003. Digitizing large fossil skeletal elements for three-dimensional applications. *Palaeontologia Electronica*, Vol. 5, Issue 2, 4: 10pp., 619KB; http://palaeo-electronica.org/2002_2/scan/issue2_02.htm.
- Wilson, G., Evans, A., Jernvall, J., and Fortelius, M. 2006. Dietary preferences of multituberculates: Preliminary inferences from dental morphological complexity patterns in muroid rodents. *Journal of Vertebrate Paleontology*, 26(3), Supplement, 139A.

Yamashita, N. 1998 Functional dental correlates of food properties in five Malagasy lemur species. *American Journal of Physical Anthropology*, 106(2):169-188.

Zuccotti, L.F., Williamson, M.D., Limp, W.F., and Ungar, P.S. 1998. Technical note: Modeling primate occlusal topography using geographic information system technology. *American Journal of Physical Anthropology*, 107(1):137-142.